J Geophys (1982) 51:153–164

Journal of Geophysics

Amplitude Study of the *Pg* Phase*

E. Banda[1], N. Deichmann[1], L.W. Braile[2], and J. Ansorge[1]

[1] Institute of Geophysics, ETH-Hoenggerberg, CH-8093-Zürich, Switzerland
[2] Department of Geosciences, Purdue University, West Lafayette, Indiana 470907, USA

Abstract. The amplitude of the *Pg* phase, as recorded in explosion seismology studies, is analyzed with the aid of synthetic seismograms. Parameters such as source frequency, low-velocity cover above the crust (sediments or weathered layer), low-velocity layers within the upper crust, velocity gradients, thickness of the gradient zone, attenuation and Poisson's ratio strongly influence the amplitude-distance pattern of the *Pg* phase. A systematic study clearly shows that different models of the continental upper crust display distinct amplitude-distance characteristics. These models could not be distinguished by travel-time interpretation alone.

In the presence of gradient zones the amplitude-distance curve shows different patterns depending on the source frequency. The higher the frequency, the more pronounced are the relative maxima in the amplitudes. The presence of a low-velocity cover at the surface accentuates the character of the amplitude-distance curves even if the cover is thin (a few hundred meters). Moreover, a low-velocity cover produces *P* to *S* conversions and multiples following the *Pg* which obscure possible secondary crustal phases. The thickness of the velocity gradient zone influences the amplitude decay and the width of the relative maxima. Low-velocity layers within the upper crust cause a faster drop-off of the amplitudes than would be expected from ray theory. Detailed *Pg* amplitude studies are thus useful in improving the knowledge of the physical properties of the upper continental crust. The application of the derived criteria to two sets of real data allow us to determine fine details of the velocity-depth function which are of great importance for the understanding of the earth's crust.

Key words: Explosion seismology – Upper continental crust – Seismic amplitude – Source frequency – Low-velocity layer – Velocity gradient.

Introduction

Understanding the fine structure and physical properties of the continental crust is one of the principle goals of explosion seismology. Interpretation of seismic refraction data using traditional travel-time methods gives only a rough picture of the velocity-depth structure. The increasing use of the ray tracing interpretation techniques and methods derived from the Herglotz-Wiechert travel-time inversion (including τ-p methods) result in velocity models of the upper crust that include velocity gradients which are very often poorly defined. In fact, layers with constant velocity, the simplest model, fit the travel-time data equally well in most cases. Healy (1963) has shown that very different velocity-depth models, from homogeneous layers to continuous gradient zones can fit equally well the travel-time data for a particular phase. However, as will be shown below, the amplitude-distance character of these models may be significantly different. At present, either very detailed travel-time information or amplitude studies are the only techniques available for accurate determination of velocity gradients in the earth's crust.

In the following discussion, we use the term upper crust for the upper 10–15 km of the crystalline continental basement lying immediately beneath the surface sediments and above the lower crustal layer. The *P*-wave velocity of the upper crust normally varies between 5.7 and 6.3 km/s. These velocities are characteristic of sialic rocks at the appropriate upper crustal temperature and pressures. The compressional seismic wave critically refracted (head wave) in the upper crust is usually called *Pg*. In explosion seismic studies, the *Pg* phase is normally recognized as the first arrival in the distance range of about 10–100 km. The notation *Pg* is also used in earthquake seismology studies but in these cases it often refers to a different phase at larger distances.

Studies of the *Pg* phase recorded in refraction profiles (Müller and Fuchs, 1976; Müller and Mueller, 1979; Banda and Ansorge, 1980; Braile et al., 1982) have shown how amplitude information can be used to greatly reduce the range of models fitting the travel-time interpretation. As refraction surveys are becoming more detailed, with closely spaced recordings and improved amplitude control, we feel that the qualitative comparisons attempted so far in most amplitude studies are not enough, and that understanding the variation of *Pg* amplitudes as a function of various parameters will provide further insight into the velocity structure of the upper crust. In turn, this information will serve as a basis for comparison with laboratory measurements and petrological studies leading to a better knowledge of the physical properties of the basement.

In this paper we discuss, on the basis of synthetic seismograms, the *Pg* amplitude-distance curves and their vari-

* Contribution No. 383 Institute of Geophysics ETH-Zürich, Switzerland

Offprint requests to: J. Ansorge

0340–062X/82/0051/0153/$02.40

ation with parameters such as frequency content of the source, presence of low-velocity cover and of low-velocity layers within the upper crust, velocity gradients, thickness of the gradient zone, attenuation (Q^{-1}) and Poisson's ratio. We also present examples of amplitude-distance modelling for observed *Pg* amplitude data from central Europe and western North America.

Methods of Computation

Synthetic seismograms can at present be calculated by a variety of methods. For our purposes we have used the reflectivity method developed by Fuchs (1968) and Fuchs and Müller (1971) with the fundamental modification by Kind (1978) and the asymptotic ray method described by Červený et al. (1977). These two methods and others have been extensively discussed in the literature (see Chapman, 1978 and Spudich and Orcutt, 1980 for reviews).

Since the objective of this paper is to describe in detail the amplitude-distance behaviour of the *Pg* wave and to understand related later arrivals (multiply reflected, refracted and/or converted), we have used mainly the reflectivity method. The modification by Kind (1978) includes these secondary effects by taking into account the free surface and placing the source in the reflectivity zone. This technique requires velocity models consisting of laterally homogeneous and isotropic layers. Velocity gradients are approximated by a stack of thin layers with small velocity contrasts. For our computations we have used thicknesses corresponding to less than one wavelength of the frequency range considered.

Record sections of the vertical component of ground displacement have been calculated for all the models with a distance interval of 5 km between 0 and 100 km (Fig. 1). Except where stated, the V_P/V_S ratio was assumed to be $\sqrt{3}$ (Poisson ratio = 0.25) and the Q_P values were fixed at 100 for the sediments or weathered layer and at 500 for the basement with Q_S equal to $4Q_P/9$. The depth of the source was fixed at 100 m depth.

All record sections were plotted with a reduction velocity of 6.0 km/s and the amplitudes of each trace were multiplied by the distance for a more accurate reading of the amplitudes (Fig. 1). Amplitudes were read taking the maximum (peak-to-peak) of the first cycle (reading the first pulse has given identical results for theoretical seismograms). Finally the amplitude readings were plotted as function of distance, as shown in Fig. 1.

The phase velocity interval used to determine the range of angles of incidence over which the reflectivity program integrates was 0.2–0.4 km/s below the minimum velocity in the models and 1.0–2.0 km/s above the maximum. This range includes all of the compressional and shear waves of interest propagating in the upper crust. The large phase velocity range leads, especially for high frequencies, to very long computer runs (e.g. for the model in Fig. 1, 23.3 min CPU time on a Cyber M0722A). However, it is worthwhile

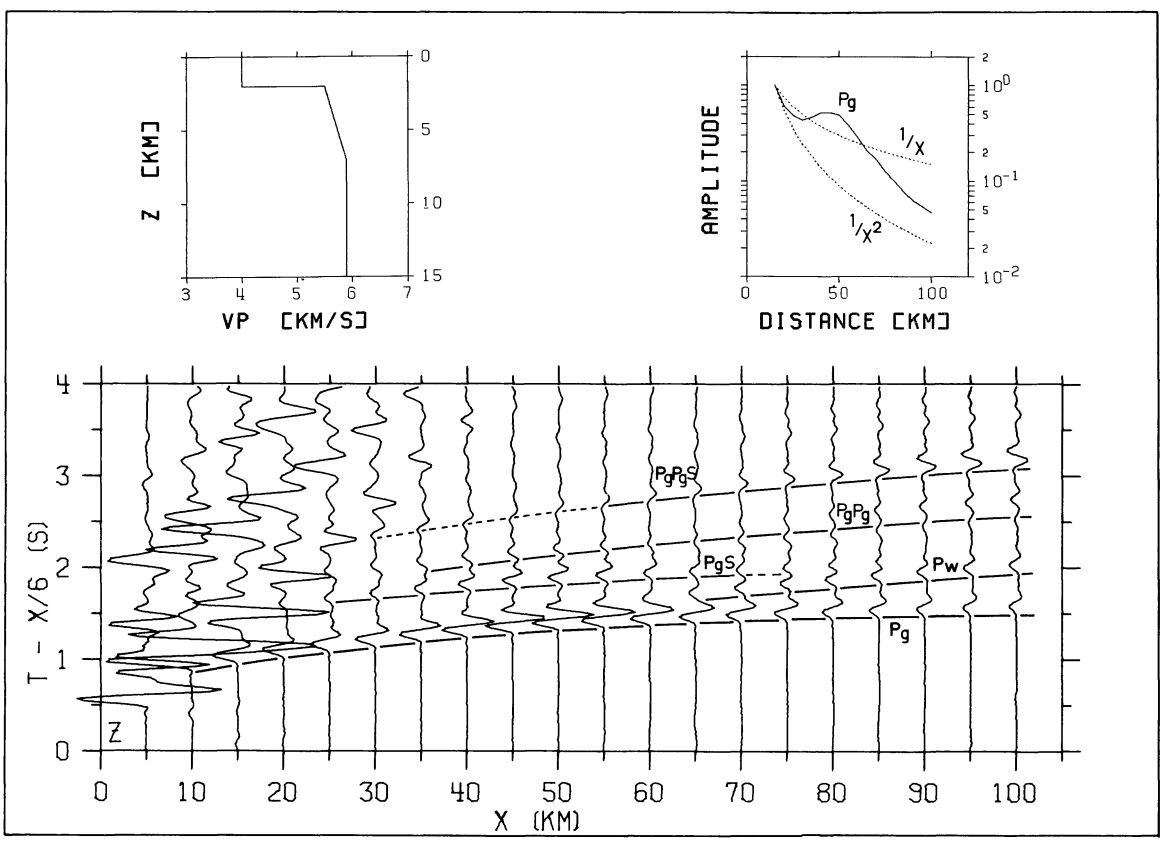

Fig. 1. Example of synthetic record-section calculated using the reflectivity method with a dominant frequency of 4 Hz for model PG11K, displayed in the *left inset*. The amplitude-distance curve (*solid line*) is shown together with the curves for $1/x$ and $1/x^2$ decays in the *right inset*. Note the prominent secondary phases: *Pw*, whispering gallery (see Červený et al., 1977), *Pg*(S), direct *Pg* converted to *S* at the base of the sediments, *PgPg*, *Pg* reflected once at the free surface, *PgPg(S)*, reflected *Pg* converted to *S*

Table 1. Model parameters

Model	Lower limit of layer (km)	Layer thickness (km)	V_P (km/s)	Number of layers	Gradient (km/s/km)
PG1	2.0	2.0	4.0	2	0.0
	15.0	13.0	6.0	5	0.0
	20.0	5.0	6.5	2	0.0
PG3	2.0	2.0	4.0	2	0.0
	15.0	13.0	5.9–6.1	5	0.015
	20.0	5.0	6.1	2	0.0
PG6	2.0	2.0	4.0	2	0.0
	15.0	13.0	5.75–6.25	5	0.038
	20.0	5.0	6.25	2	0.0
PG11	2.0	2.0	4.0	2	0.0
	15.0	13.0	5.5–6.5	5	0.077
	20.0	5.0	6.5	2	0.0
PG11K	2.0	2.0	4.0	2	0.0
	7.0	5.0	5.5–5.885	5	0.077
	20.0	13.0	5.885	3	0.0
PG11KK	2.0	2.0	4.0	2	0.0
	10.0	8.0	5.5–6.12	10	0.077
	20.0	10.0	6.12	2	0.0
PG11L	2.0	2.0	4.0	2	0.0
	7.0	5.0	5.5–5.885	5	0.077
	12.0	5.0	5.5	1	0.0
	20.0	8.0	6.3	1	0.0
PG11LL	2.0	2.0	4.0	2	0.0
	10.0	8.0	5.5–6.12	8	0.077
	15.0	5.0	5.5	1	0.0
	20.0	5.0	6.3	1	0.0
PG12	2.0	2.0	4.0	2	0.0
	15.0	13.0	6.1–5.9	5	−0.015
	20.0	5.0	6.5	2	0.0
PG22	2.0	2.0	4.0	2	0.0
	15.0	13.0	5.3–6.7	5	0.108
	20.0	5.0	6.7	2	0.0
SULZ3	1.0	1.0	4.5	2	0.0
	1.3	0.3	4.8–5.6	1	2.67
	5.0	3.7	5.6–5.9	5	0.081
	10.0	5.0	5.9–6.1	7	0.04
	21.0	11.0	6.1	2	0.0
SULZ4	1.0	1.0	4.3	2	0.0
	1.3	0.3	4.8–5.6	1	2.67
	6.3	5.0	5.6–6.0	6	0.08
	17.0	10.7	6.0	2	0.0
SULZ6	1.0	1.0	4.6	2	0.0
	5.7	4.7	5.6–5.95	7	0.074
	8.2	2.5	5.95–6.0	4	0.02
	17.0	8.8	6.0	1	0.0
SULZ7	1.0	1.0	4.6	2	0.0
	5.7	4.7	5.6–5.95	7	0.074
	7.0	1.3	5.95–5.98	3	0.023
	17.0	10.0	5.98	1	0.0

performing these computations to reveal the influence of the sediments. Many tests were run before choosing the best illustrative models for the purpose of this paper, which are listed in Table 1.

To compare the performance of the reflectivity method

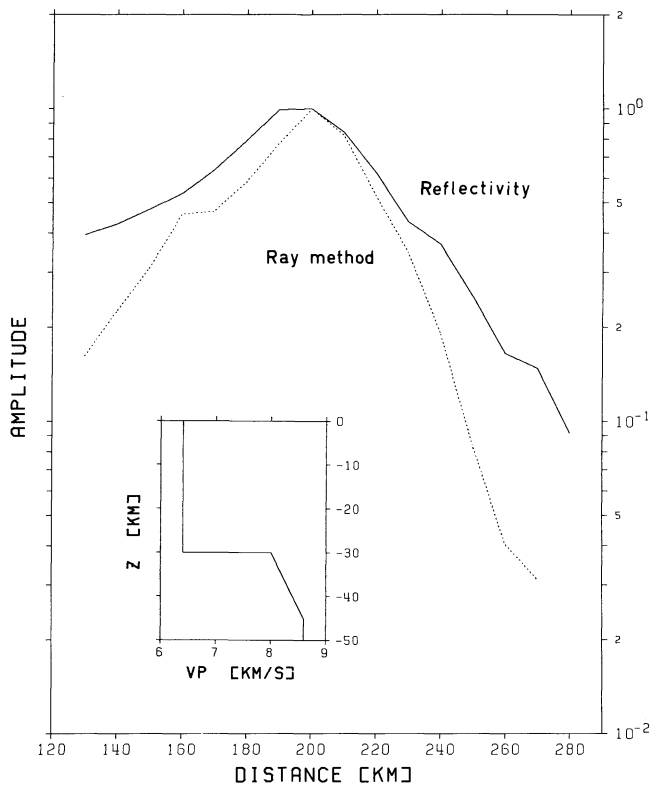

Fig. 2. Amplitude-distance curves (peak-peak) of *Pn* phase for model EC4 (Červený, 1979) computed using reflectivity (*continuous line*) and using ray-method (*dotted line*)

with the asymptotic ray theory method, we started by determining the amplitude-distance curves for one of the models published by Cerveny (1979) for which he used both methods (Fig. 2). Although this case deals with a gradient zone in the upper mantle, the situation is analogous to a gradient zone in the upper crust with a sedimentary layer above. The ray method obviously sharpens the peak of the amplitude-distance curve. This is because the asymtotic ray method represents a "high frequency approximation" to the wave equation (Červený et al., 1977; Chapman, 1978). As is shown below, similar results were obtained from other computations in this study. The ray method is inexpensive and for much of the available data and some crustal models, which can also include lateral inhomogeneities, this approximation is accurate enough. For more detailed studies, in which the models can be approximated by flat homogeneous layers, the reflectivity method is more appropriate and has therefore been used in this paper.

The synthetic seismograms computed in this study represent ground displacements instead of ground velocities, as measured in observed seismograms. As shown in the example in Fig. 3, for which both velocity and displacement were calculated, the difference in the amplitude-distance behaviour is not significant. At least for the models presented here, the results from displacement can thus be applied directly to observed velocity data. Moreover, it should be noted that the dominant frequency used in displacement computations is increased when the displacement seismograms are differentiated to obtain velocity (see spectra in Fig. 3).

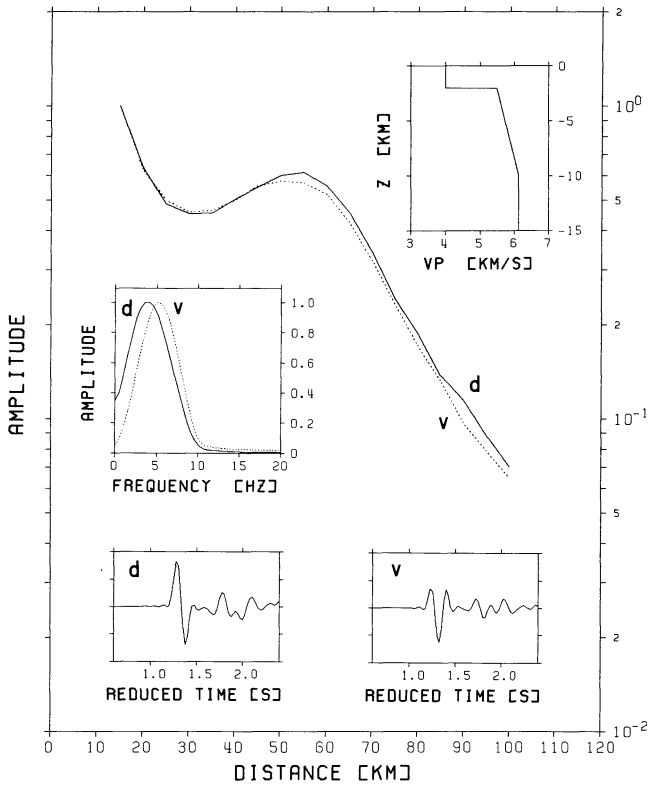

Fig. 3. Comparison of amplitude-distance curves of displacement (*continuous line*) and velocity (*dotted line*) seismograms for model PG11KK (*upper right inset*). The corresponding spectra show the frequency shift between displacement and velocity signals. The *bottom insets* show the signals (at 35 km) for displacement and velocity; the intervals used to calculate the spectra are marked by *vertical bars*

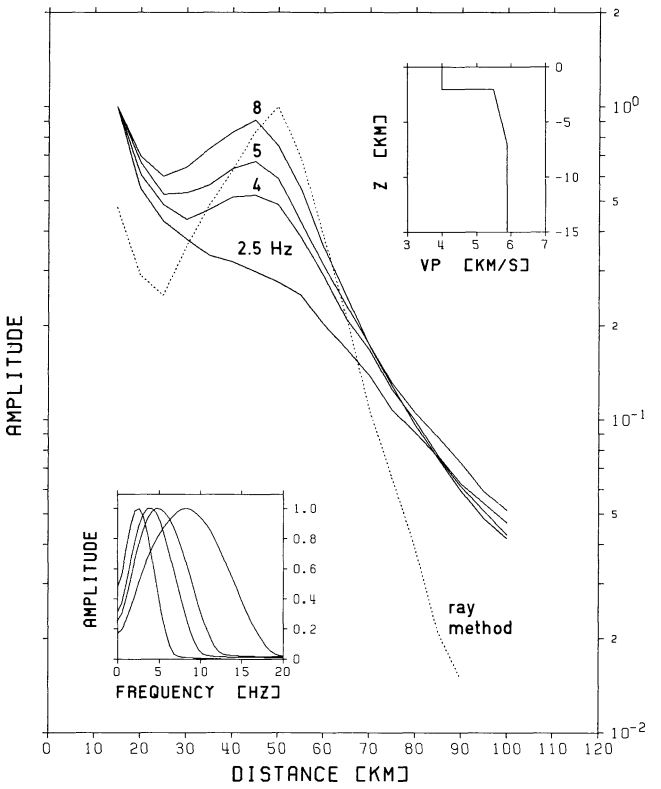

Fig. 4. Amplitude-distance curves for model PG11K (*upper right inset*) for frequencies of 2.5, 4, 5 and 8 Hz (Fourier spectra in the *lower inset*) computed using reflectivity method (*continous lines*). *Dotted line* corresponds to ray-method computation with program SEIS4

Discussion of Model Parameters

Source Frequency

The frequency content of seismic refraction data varies from about 2 Hz to more than 20 Hz depending on the shooting technique, charge size, frequency response of the instrument and local geological environment. Comparison of the shape of the amplitude-distance curves for low frequency source signals ($\sim$2 Hz) with those for high frequency ($\approx$8 Hz) shows significant differences when velocity gradients are truncated at shallow depth or low-velocity layers are present in the model. For that reason we have computed most of the models for frequencies 2–8 Hz.

Figure 4 shows an example of the results for model PG11K computed for 2.5, 4, 6 and 8 Hz dominant frequencies. The fact that the velocity structure of the upper crust changes, from a positive gradient (0.077 km/s/km) to zero gradient at 7 km depth produces a different response of the medium depending on the source frequency. The variation of amplitude with distance is more pronounced at the higher frequencies. As discussed in more detail below, this is due to the fact that shorter wavelengths are affected mainly by the focusing effect of the gradient zone, thus producing strong relative amplitude-maxima at a distance of 45 km. At the same distance, longer wavelengths are already affected by the homogeneous layer beneath the gradient zone. Higher frequencies are thus more informative in amplitude studies.

For the same model, amplitudes were computed with the asymptotic ray theory and are also displayed in Fig. 4. As was to be expected, the ray method works reasonably well for high frequencies, although the slope of the amplitude decay is somewhat enhanced. Asymptotic ray theory accounts for the influence of different frequencies on the amplitudes of waves reflected at first order discontinuities (Červený et al., 1977) but not for waves refracted from a gradient zone (Banda, 1979). Therefore, if we are dealing with good quality data, suitable for amplitude studies, it is of fundamental importance to compute the theoretical seismograms using the reflectivity, or other wave theory method, with a source which has a dominant frequency similar to that of the experimental data.

Thickness and Velocity Structure of Sediments

Qualitative differences in the character of the wave field due to the presence of sediments are well known. Their influence was studied quantitatively with models which are identical except for the velocity structure of the sediments.

Figure 5 shows the results for models with 0, 0.2, 2 and 5 km of sediments overlying an upper crust containing a velocity gradient of 0.077 km/s/km. Beyond about 60 km the shapes of the amplitude-distance curves are essentially identical. The most important difference is that even for models with as little as 0.2 km of sediments, a relative maximum of the amplitude curve is observed which is missing

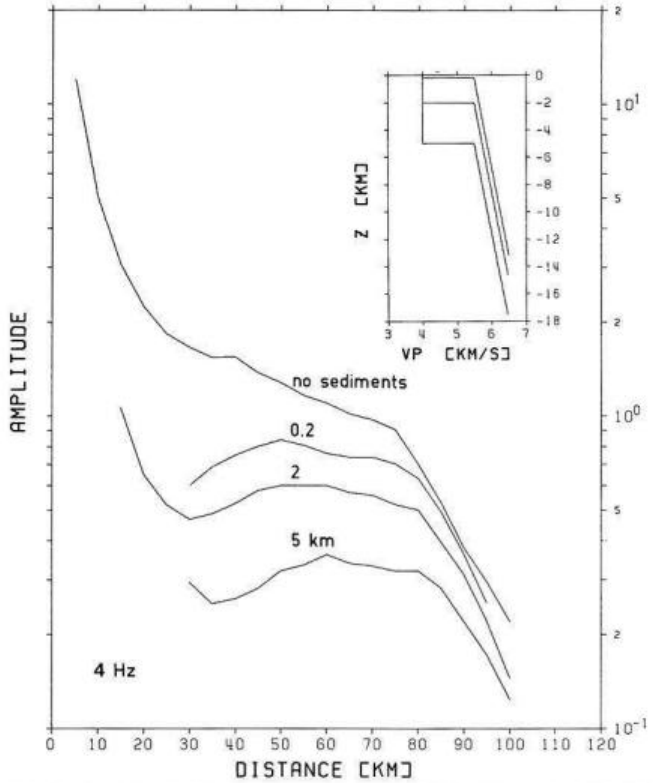

Fig. 5. Amplitude-distance curves for model PG11 with 0.0, 0.2, 2.0 and 5.0 km of low-velocity material (*inset upper right*) overlying the basement

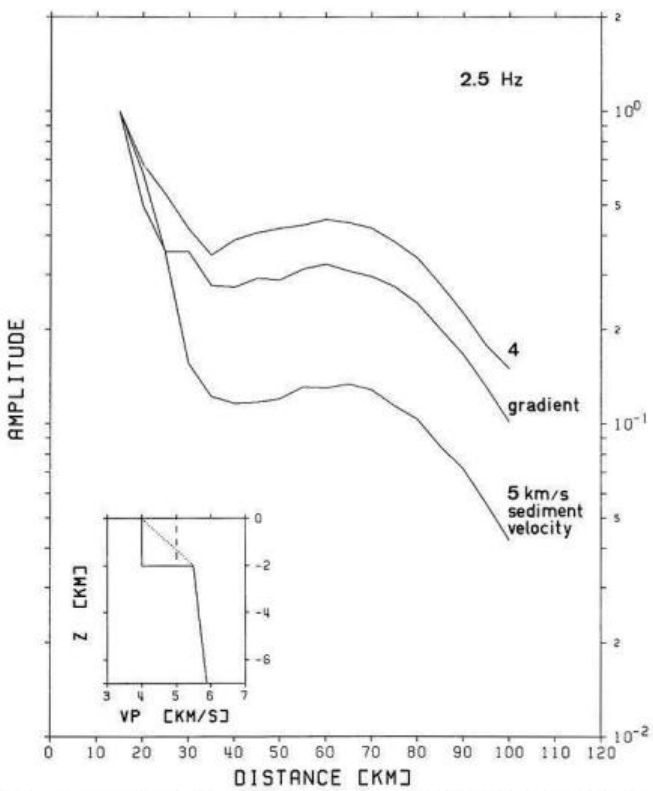

Fig. 6. Amplitude-distance curves for model PG11 (2.5 Hz) with different velocity structures of the low-velocity cover of the basement (*inset lower left*)

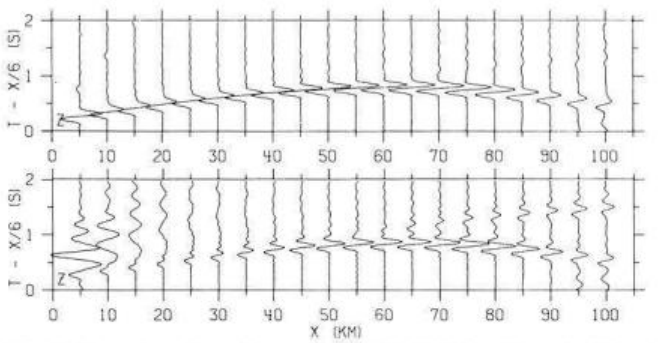

Fig. 7. Record-sections for model PG11 (4 Hz) with and without low-velocity cover (0.2 and 0.0 km, lower and upper sections respectively). Note the difference in the wave field of secondary arrivals (see also Fig. 1)

for the model without sediments. We interpret this as an effect of the change of the angle of incidence affecting the transmission coefficient. On the other hand, models with a low-velocity cover alone and without a gradient in the upper crust do not have a relative amplitude maximum.

Results for models with different velocity structures in the sediments are displayed in Fig. 6, which show that there is no significant difference in the overall shape of the *Pg* amplitude-distance curves. However, the level of the amplitudes at the local maximum around 60 km relative to the amplitudes at 15 km is lower for sediments with a velocity of 5 km/s than for those of 4 km/s or for sediments with a velocity gradient starting with 4 km/s at the surface. This again is due to the fact that the angle of incidence is steepened by the lower velocity at the surface, thus producing higher *P*-wave amplitudes on the vertical component seismograms studied here.

As a result, we can state that any influence of the thickness and velocity structure of the sedimentary layer on the amplitude-distance behaviour of the first cycle of the *Pg* phase is restricted to shorter distances. However, the total wave fields for models with and without sediments are radically different. Reverberations within the sediments and *P* to *S* conversions result in conspicuous seismic phases that appear after the *Pg* phase (Fig. 7, see also Fig. 1).

Thickness of Gradient Zone and Low-Velocity Layers

Significant differences in the amplitude-distance curves for models having the same gradient but different thickness of the gradient zone are shown in Fig. 8. The models include structures with a continuous gradient between 2 and 15 km (model PG11), 2 and 10 km (model PG11KK) and 2 and 7 km (model PG11K) on top of a half space. A decrease in the thickness of the gradient zone leads to a faster drop-off of the amplitudes with distance.

The introduction of a low-velocity layer below a gradient zone between 2 and 7 km and 2 and 10 km (models PG11L and PG11LL) show another interesting effect. A significant shift of the maximum and a change in the slope of the amplitude decay is evident when a low-velocity layer is present at the same depth at which the gradient is terminated (compare PG11K and PG11L in Fig. 8).

The influence of the frequency content of the source in the presence of a low-velocity layer is shown in Fig. 9. The main effects are to sharpen the maximum and to shift

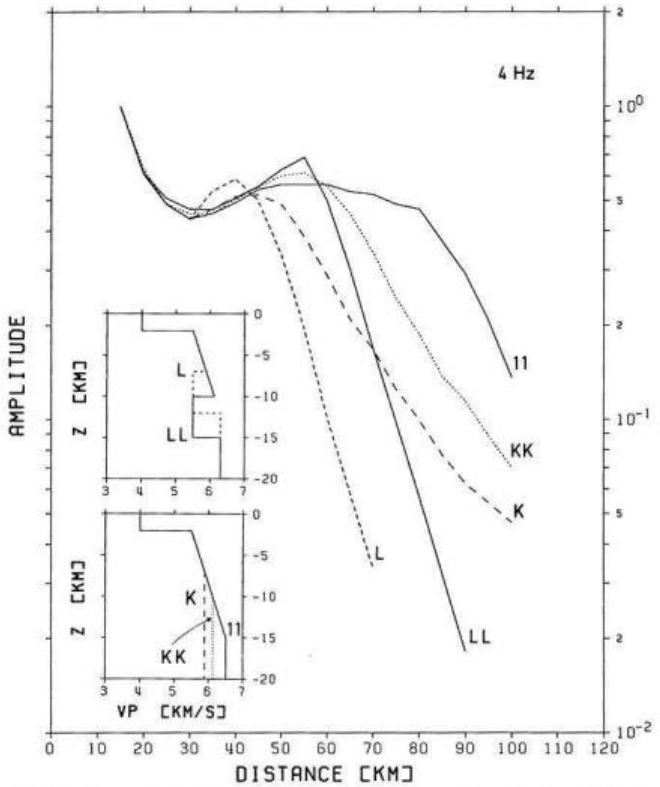

Fig. 8. Amplitude-distance curves for models PG11, PG11K, PG11KK with variable gradient zone thickness (*continuous, dashed and dotted lines*, respectively in the *lower inset*) and PG11L and PG11LL with low-velocity layer at different depths (*dashed and continuous lines*, respectively, in the *upper inset*) computed for a frequency of 4 Hz

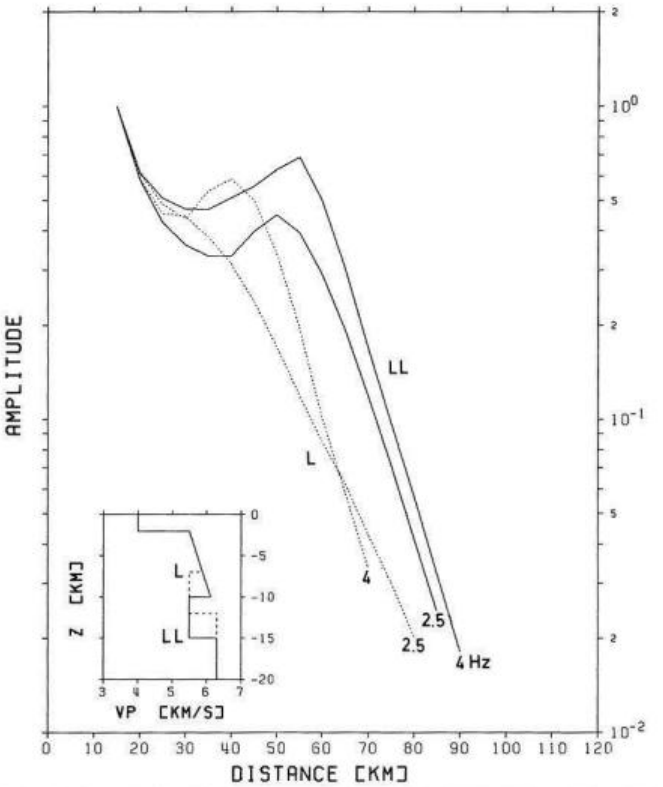

Fig. 9. Amplitude-distance curves for models PG11LL and PG11L (*continuous* and *dotted lines* respectively, in the *inset*) computed for 2.5 and 4 Hz

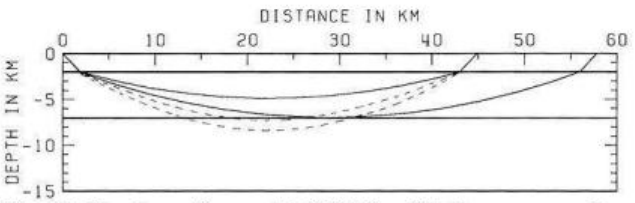

Fig. 10. Ray-trace for model PG11K, with the ray emerging at 45 km and the ray grazing the lower boundary of the gradient zone emerging at 58 km (*solid curves*). The *lower dashed curve* shows the edge of the first Fresnel-zone (corresponding to a phase shift of $T/2$) while the *upper dashed curve* corresponds to a phase shift of $T/4$ for a signal with 4 Hz dominant frequency

it to larger distances as the frequency is increased. Model PG11L peaks very smoothly for 2.5 Hz at about 30 km whereas it peaks sharply at 40 km for the higher frequencies. The waves behave as if they "sense" the low-velocity layer well before this would be expected from ray considerations. To illustrate the effect of the truncated gradients, the ray tracing for model PG11K is shown in Fig. 10. Here, even though the gradient zone is terminated at a depth of 7 km, we observe rays emerging at distances out to 58 km, which is in disagreement with the results from these amplitude calculations. As stated above, a decrease in thickness of the gradient zone causes the Pg-amplitude drop-off to occur at smaller distances than expected. For models PG11K and PG11L, in which the gradient zone is terminated at 7 km depth, the amplitudes start deviating from those of model PG11, whose gradient extends down to 15 km, at distance as short as 45 km. As is shown in Fig. 10 rays arriving at this distance reach a maximum depth of only 4.9 km, which is well above the bottom of the gradient zone. In fact, the distance between the turning point of the ray and the bottom of the gradient zone is greater than one wavelength (about 1.5 km at 4 Hz). This phenomenon, which can not be explained by geometrical ray theory, is analogous to the Fresnel-zone effect in the case of electromagnetic waves: the energy arriving at a receiver is due not only to the ray propagating with minimal travel-time, but, as a consequence of Huyghens' principle, consists of difractions interfering with each other, whose travel-times are greater than that of the direct wave (Born, 1933). Modifications of asymptotic ray theory which take this effect into account have been introduced by various authors (see Spudich and Orcutt, 1980 for a review). In particular, Wiggins (1976) approximates the wave behaviour by envisaging the energy transported by a ray as being distributed over a disk travelling with that ray, and constructs a synthetic seismogram by summing the contribution of neighbouring rays as their disks intersect the surface at the distance of interest. As can be seen from the dashed ray-paths in Fig. 10, the first Fresnel zone, which contains the most significant contributions to the amplitude of the signal, extends to a depth beyond the limit of the gradient zone for energy arriving at a distance of 45 km. Thus, changes in gradient will influence the amplitudes of waves with longer periods at smaller distances than those with shorter periods. This is also the reason for the marked shift of the amplitude peak in models PG11L and PG11LL between

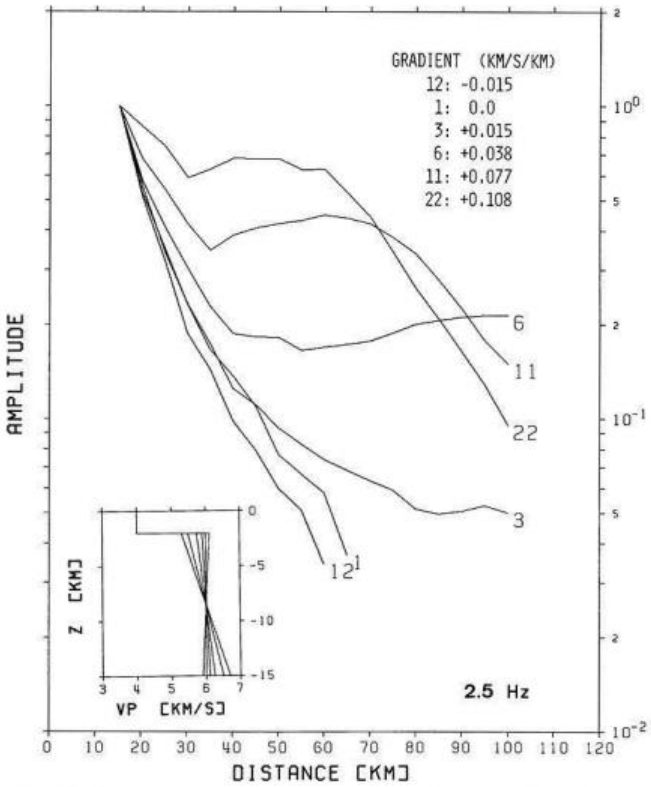

Fig. 11. Amplitude-distance curves for models PG12 (negative gradient). PG1 (no gradient) and PG3, PG6, PG11 and PG22 (positive gradients) for a frequency of 2.5 Hz (see Table 1 for model specifications)

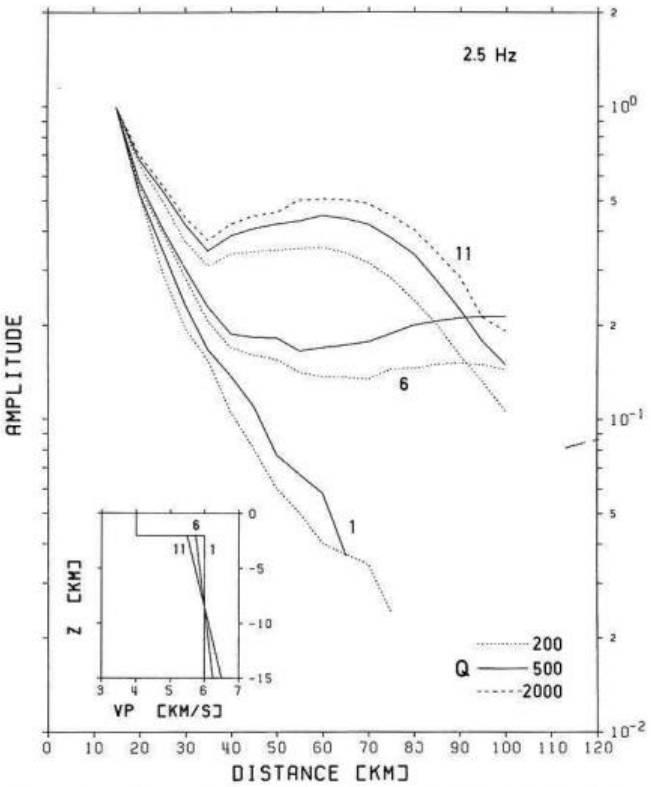

Fig. 12. Amplitude-distance curves for models PG1, PG6 and PG11 (see *inset* and Table 1) for $Q=500$, continuous lines, $Q=200$, *dotted lines* and $Q=2000$ (*dashed line* for model PG11)

2.5 and 4 Hz, and for the frequency dependence shown in Fig. 4.

Reflections originating from the low-velocity layer have also been studied. Our results do not differ from those published by Braile and Smith (1975), Smith et al. (1975) and further modified by Banda (1979): the reflection from the top of the low-velocity layer will only be seen as a separate phase when the upper crust has a very small or zero gradient, the frequency is high enough and the transition is nearly a first order discontinuity. In this case the interference of *Pg* with the reflection changes the *Pg* amplitudes at larger distances (this has not been studied in detail in this paper). If the above mentioned conditions are not fulfilled the *Pg* amplitudes will barely be affected by the reflection from the top of the low-velocity layer.

Variation of Gradients

It is well known that even a slight positive velocity gradient greatly influences the amplitude of refracted phases (Červený, 1966; Hill, 1971). Thus, we have tried to vary systematically the velocity gradient in the basement models in order to determine the corresponding amplitude-distance curves. We have arbitrarily chosen the gradient to be linear. Amplitudes for models with various gradients between -0.015 and 0.108 km/s/km were computed and are shown in Fig. 11. From a comparison with a calculation for model GP11 at higher frequency and from the discussion in the previous section, it can be stated that, although these curves were calculated for 2.5 Hz, they are also representative of higher frequencies as long as the gradient zones extend to sufficient depth. The results shown in Fig. 11 illustrate that small positive velocity gradients in the upper crust will be resolvable by amplitude measurements on reasonably good experimental data. For example, the amplitude-distance characteristics of Models PG1 and PG6 are significantly different although the velocity structure differs only by the presence of a small (0.038 km/s/km) gradient in Model PG6.

Attenuation (Q)

We have tested models with Q values for compressional waves of 200, 500 and 2000 for the upper crust to investigate the influence of attenuation upon the amplitude of the *Pg* wave. The curves shown in Fig. 12 are not sufficiently distinct for us to infer apparent Q from *Pg* amplitude calculations. As already demonstrated by Hill (1971) a slight change in the gradient could make up for the differences shown in Fig. 12 without taking the attenuation into account. To estimate Q in the basement one could use the method proposed by Braile (1977) which requires that the *Pg* amplitudes be modelled simultaneously with the amplitudes of the reflection from the bottom of the upper crust. Alternatively, if the geometrical spreading factors are sufficiently well known, and the band-width of the source is broad enough, it is conceivable that spectral ratio methods (see Båth, 1974 for a review) might be adequate to infer Q in the upper crust.

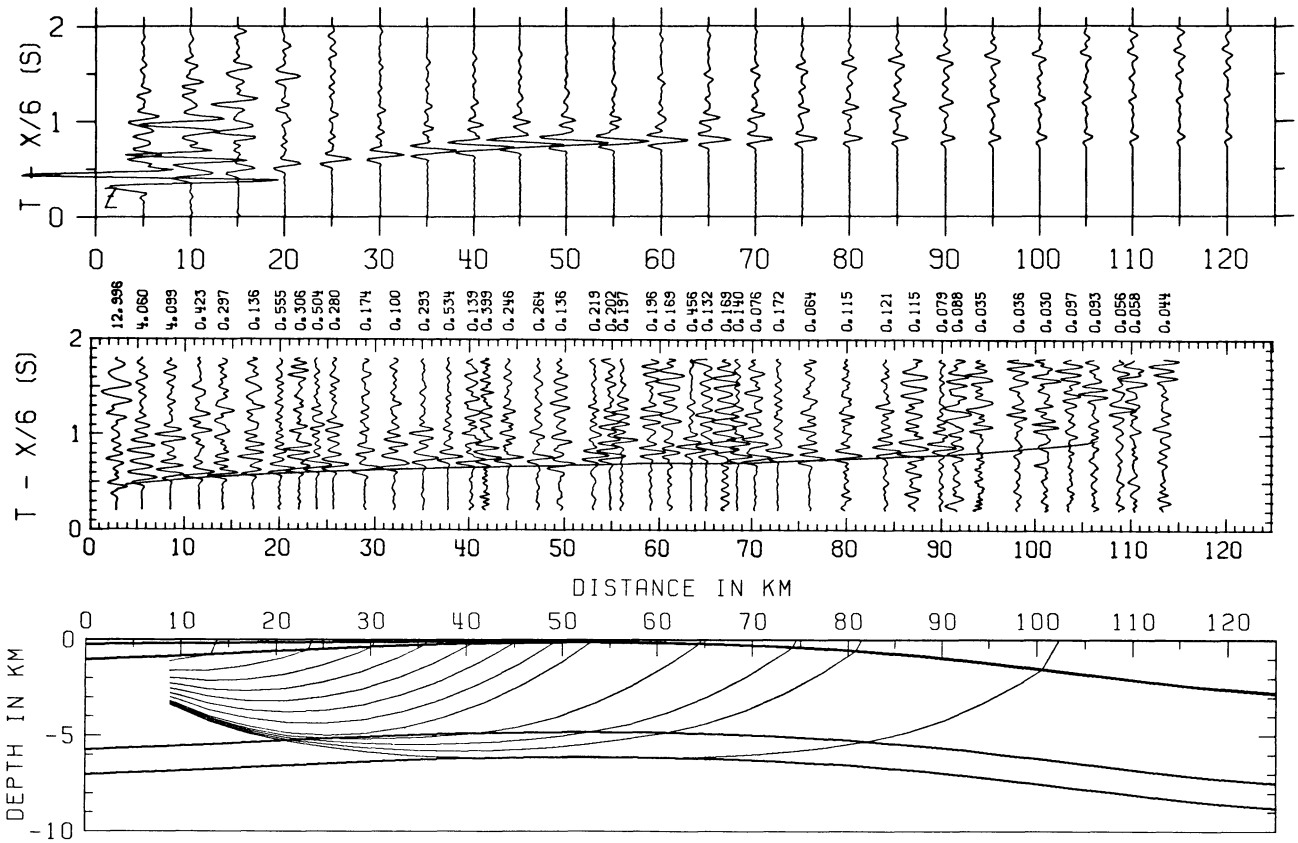

Fig. 13. *Bottom*. ray-trace for model Sulz-7. Note vertical exageration of model plot. *Middle*. record section of Sulz-south data, vertical component, bandpass filtered 8–16 Hz, trace normalized. Travel-time curve corresponds to ray-trace below. *Top*. synthetic record section of flat layer approximation of model Sulz-7 (see Fig. 14 and Table 1) vertical component velocity amplitude multiplied by distance

Poisson's Ratio (σ)

Seismic velocity studies of the crust show that a Poisson ratio of 0.25 is in general a good average. However, in some cases strong deviations from this value have been found. The influence of σ has been studied for a few models with values 0.2–0.35. The resulting amplitude-distance curves do not differ significantly from each other. Only curves for models involving a sudden change of σ at a discontinuity produce distinct features in the *Pg* versus reflection amplitude ratio as already shown by Olsen et al. (1979).

Examples of Data from the Black Forest (Germany) and the Basin and Range (U.S.A.)

Between 1974 and 1980 several quarry blasts near Sulz, southern Germany, were recorded along a 113 km long profile running south along the eastern margin of the Black Forest into the Swiss Alpine foreland. The first 2 s of the resulting seismic record-section are shown in Fig. 13 together with the travel-time curve corresponding to the ray-trace model in the lower part of the figure. The ray tracing was performed using the method of Gebrande (1976).

The velocity structure of the sediments (including a wedge of late Paleozoic and early Mesozoic sediments with *P*-velocity of 3.8 km/s between 0 and 40 km) and the shape of the basement/sediments boundary were modelled to fit the available bore-hole data (Buechi et al., 1965; Boigk and Schoeneich, 1968; Lemcke et al., 1968). The velocity structure of the basement was then adjusted until the general shape of the travel-time data was matched. No attempt was made to model the local variations in sedimentary structure and basement depth which produce the small time discrepancies, limited to one or two consecutive records. This applies particularly to the local anomaly between 94 and 101 km which, because of the poor signal to noise ratio, cannot be resolved with these data alone.

For plotting convenience, the seismograms in Fig. 13 were trace normalized. The peak-to-peak amplitudes of the first cycle were multiplied by the scale factor marked above each seismogram to obtain the true particle velocity values in μm/s. The amplitude data for the *Pg* phase are plotted as crosses with corresponding shot and station numbers in Fig. 14.

The size of shot number 1 was only 700 kg while the others were around 2,000 kg, so that the corresponding amplitude values were multiplied by a correction factor of 1.4, equal to the cube root of the charge ratio, which seems to be appropriate for this specific quarry. The remaining scatter seems to be independent of the shots, and although it amounts to about a factor of two, the data define an amplitude-distance behavior characterized by a rapid decrease in the first 20 km, a local maximum at about 40 km and a smooth decay out to about 100 km.

In order to be able to apply the reflectivity method to the data, the curved layers derived from the ray-tracing technique were approximated by flat layers in model

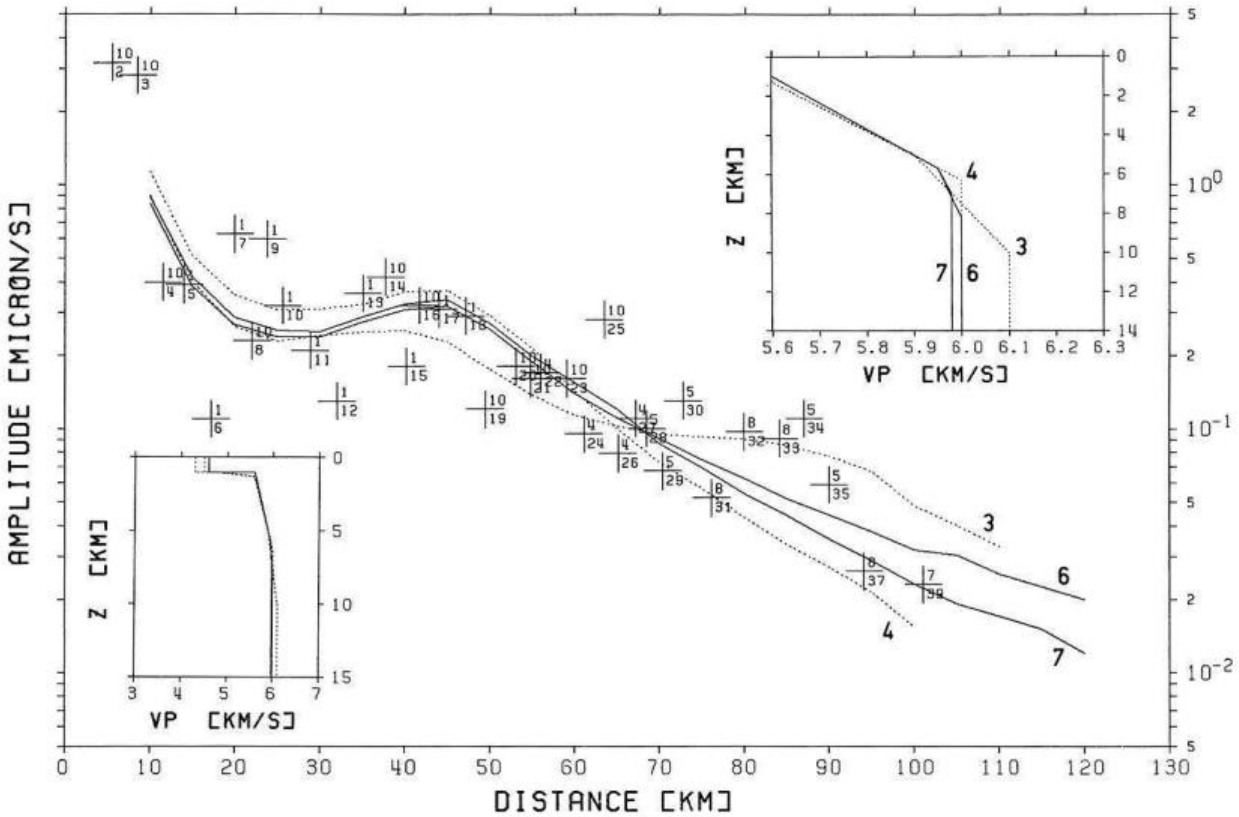

Fig. 14. Amplitude data of Sulz-South record section (Fig. 13) (*crosses* with shot and station numbers) and amplitude-distance curves for the four models shown in the *lower inset* and listed in Table 1. *Top inset* shows an enlarged view of the gradient zones of the four models

number 7 (insets in Fig. 14 and Table 1) and the sediments were simplified to a single layer. The resulting synthetic record section (vertical ground velocity with a dominant frequency of 8 Hz) is reproduced at the top of Fig. 13. The offset of the calculated amplitude-distance curve as a whole was adjusted to the experimental data by a least-squares method (Fig. 14, curve 7). For three other ray-trace models which satisfy the travel-time data equally well, amplitude-distance curves were calculated in the same way and plotted in Fig. 15 together with their velocity-depth functions. This illustrates some of the possible model variations. A comparison between models 3 and 4 shows how a second gradient zone of sufficient strength and extent can significantly increase the distance at which the amplitude decay occurs. Models 6 and 7 illustrate the effect of small changes in the extent of a second zone with slight gradient. The logarithmic standard deviations of data points from these curves range between 0.23 and 0.27, which correspond to amplitude factors of 1.7 and 1.9 respectively. The amplitude-distance behaviour of the models presented here do not differ from each other sufficiently to be able to discriminate between them on the basis of this data alone. However, as the insets in Fig. 14 show, the velocity-depth variations of these models are very small, so that the results are good evidence for a strong gradient (0.07–0.08 km/s/km) in the upper 5–6 km of the basement.

It should be noted that computational techniques restrict us to consideration of flat-layered models for the amplitude modelling even though small lateral variations are evident in the travel-time model for the Sulz data as shown in Fig. 13. Shooting up-dip over the first 50 km and down-dip beyond that distance will have a slight focusing effect on the rays, thus contributing somewhat to the observed relative amplitude maximum at that distance. However, because the lateral changes in velocity structure indicated in Fig. 13 are small (note that the model is plotted with 2× vertical exageration) and because the positive velocity gradients in the flat-layered models which satisfy the amplitude data also fit the travel-time data modelled with a curved sediment-basement boundary, we anticipate that the amplitude-distance effects of the two-dimensional structure will be negligible.

A very different amplitude-distance character of the *Pg* phase is observed for the Basin and Range province of the tectonically active western North American continent. A *Pg* data-set from this region was analyzed for this study. The seismic records are from the northern Basin and Range (NBR) (shotpoints Mountain City, Eureka and Elko) in Western United States and were originally studied by Hill and Pakiser (1966) and presented by Prodehl (1970, 1979).

Partial record sections emphasizing the *Pg* arrivals for the NBR data are shown in Fig. 15. The record sections are from Prodehl (1979) and the travel-time curves shown are the results of ray-trace modelling by Fauria (1981). Amplitudes of the *Pg* phase were read from the sections shown in Fig. 15 and corrected for plot scaling factors using the calibration signals presented on the original sections (Prodehl, 1979). The *Pg* amplitudes were adjusted to account for the differing shotpoints and plotted as a function of distance in Fig. 16. Although there is considerable

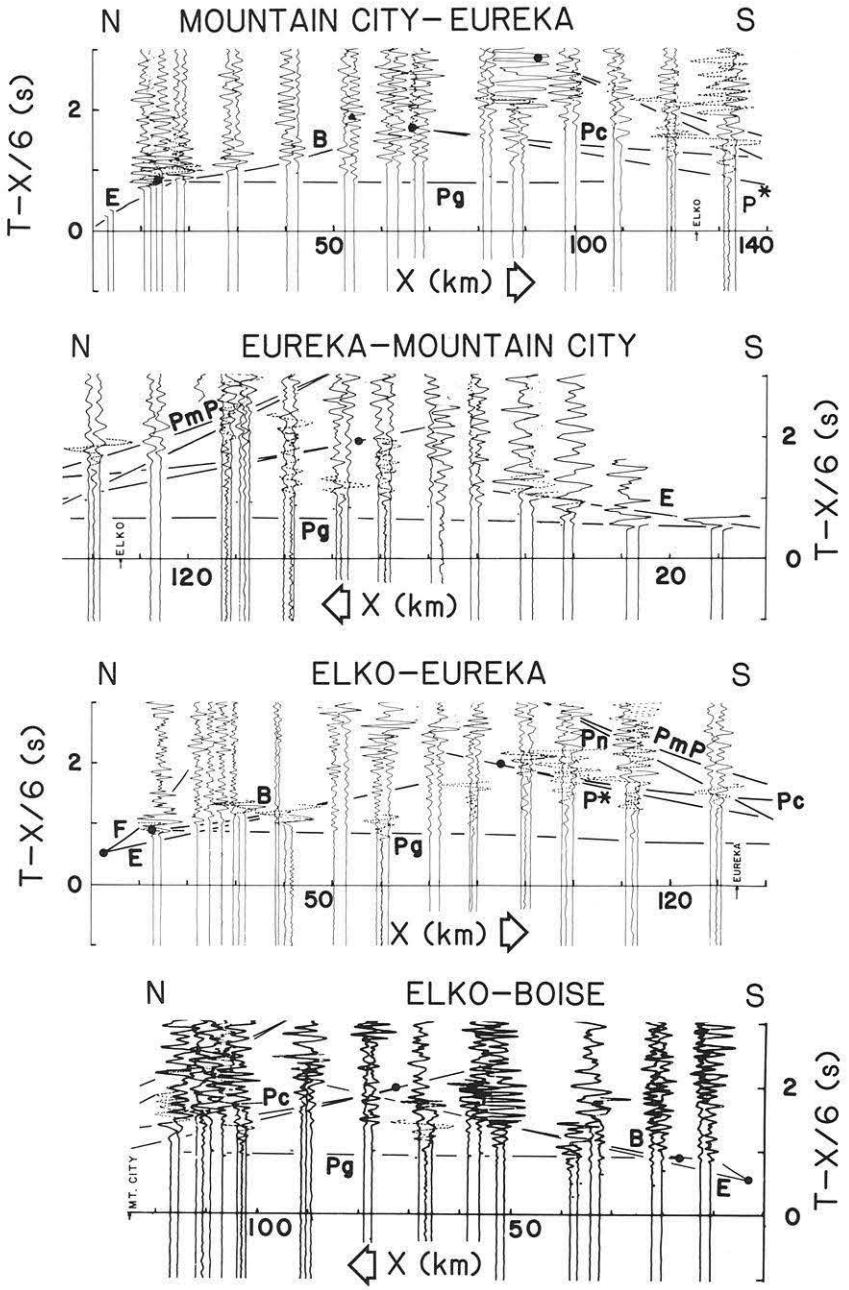

Fig. 15. Partial record sections of the *Pg* phase for the northern Basin and Range province. Travel-time curves shown are the result of ray-trace modelling by Fauria (1981)

scatter in these data (the range is illustrated by the shaded area of the plot) it appears that *Pg* amplitudes for the NBR decay rapidly with distance and do not display the local maximum which was characteristic of the Sulz data and which indicated a velocity gradient. In fact, the NBR *Pg* amplitude data are fitted best by the PG1 model consisting of homogeneous upper crust. The scatter in the data shown in Fig. 16 and the fact that the data represent a compilation from several different refraction lines preclude more detailed analysis. Note that the very small positive or negative gradients (less than that for model PG3) and virtually any Q value could be present in the upper crust of the NBR based on these data alone. However, because no strong gradient or low-velocity effects are observed in the amplitude distance data, the upper crust in the NBR appears to be nearly a homogeneous velocity layer.

Conclusions

The fine structure of the continental basement, i.e. the distribution of physical parameters with depth, can reveal significant aspects of the crustal evolution and the interaction of different crustal units as well as its thermal and compositional history. Very often the upper part of the crust does not show pronounced interfaces with discontinuities in velocity and density. Vertical incidence reflection cannot resolve velocity structure in the absence of distinct impedance boundaries. On the other hand, combined travel-time and amplitude analysis of refraction data can give more detailed insight into the velocity structure. Therefore combined reflection and refraction surveys should be carried out in crustal investigations.

A representative velocity-depth structure requires either

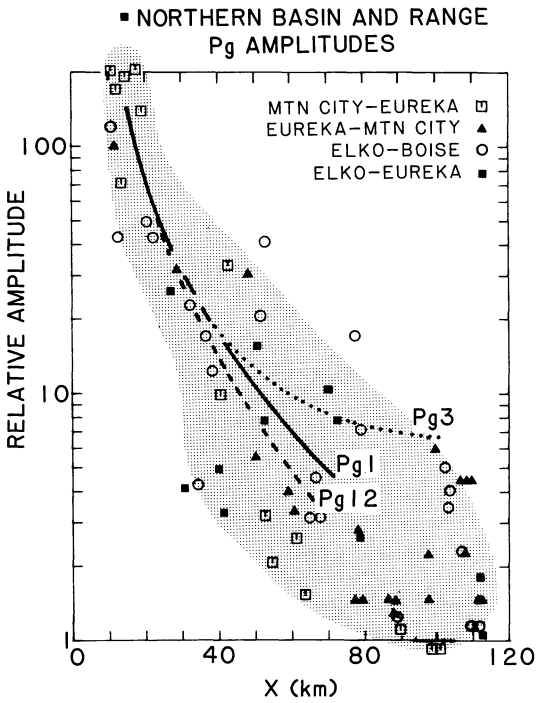

Fig. 16. Amplitude-distance data for the *Pg* phase for the NBR data shown in Fig. 15. The *shaded region* represents the range of scatter of the data points. Theoretical amplitude-distance curves calculated by the reflectivity method are shown for models PG1, PG3 and PG12 (Table 1)

detailed and highly accurate travel-time data, i.e. a spacing of observation points on the order of a few hundred meters, or a combination of travel-time and reliable amplitude data obtained from an average record spacing of a few kilometers. The following conclusions drawn from this study can help to achieve a better interpretation of the amplitude data and hence lead to a more reliable estimate of velocity-depth structure of the upper continental crust.

1. The frequency content of the source is a critical parameter when gradient zones and/or discontinuities of velocity are present. Higher frequencies produce more pronounced variations of amplitudes with distance. The amplitude variations are likely to be resolvable within the scatter of the data and thus high frequency source signals lead to better resolution.

2. A low-velocity cover of the basement accentuates relative maxima in the amplitude-distance curve when velocity gradients are present in the crystalline upper crust. Layer thicknesses of only 0.2 km, i.e. even weathered layers, can cause this effect. In addition, multiple reflections, refractions and conversions in the low-velocity cover contribute considerably to a complicated wave field following the initial *Pg* arrival and probably make later arrivals from deeper parts of the crust undetectable.

3. Reflections from the top of a low-velocity layer within the upper crust will affect the *Pg* amplitudes by interference only if they are strong enough. This requires low gradients in the basement above, a first order discontinuity at the bottom of the upper crust and a high frequency source signal.

4. The increasing thickness of the gradient zone in the basement reduces the amplitude decay with distance and broadens the width of the relative amplitude maximum.

5. The *Pg* amplitudes decay with distance much faster in the presence of a low-velocity layer than would be expected from geometrical ray theory.

6. Reliable *Pg* amplitude data, characterized by a continuous decrease, or a steady value over some distance or even a local maximum, allows us to distinguish between homogeneous constant velocity layers and various gradient zones in the upper crust.

7. Apparent Q values cannot be extracted from the amplitude distance behaviour of *Pg* data alone.

8. Synthetic seismogram calculations based on asymptotic ray theory can be used only as a first approximation to determine detailed velocity depth structures.

These results, of course, apply only to a crust which can be approximated by lateraly homogeneous models. Focusing effects due to lateral heterogeneities may completely mask the amplitude-distance behaviour due to vertical structures and must be studied by other methods.

Acknowledgements. This work was initiated when one of us (LWB) was on sabbatical leave at the Institute of Geophysics, ETH-Zürich, Switzerland. We thank Rainer Kind for providing a copy of his modified reflectivity programme. Claus Prodehl provided original copies of some of the seismic record sections. Partial support for LWB was provided by Office of Naval Research Earth Physics Program contracts N00014-75-C-0972 and N00014-82-K-033 and by the U.S. Geological Survey Geothermal Exploration Program grant No. 14-08-0001-G-674. The help of Dieter Emter in organizing the quarry blasts at the shotpoint Sulz is gratefully acknowledged. We are also grateful to Erhard Wielandt for helpful discussions regarding the Fresnel-zone effect and to Walter Mooney for his contribution to the phase identifications in Fig. 1. Agustin Udias, Walter Mooney, Robert B. Smith and Josep Gallart critically read the manuscript.

References

Banda, E.: Perfiles Sísmicos Profundos en Corteza Continental. Estructura de la Corteza y Manto Superior en las Cordilleras Béticas. Ph D.Thesis, University of Barcelona 1979

Banda, E., Ansorge, J.: Crustal structure under the central and eastern part of the Betic Cordillera. Geophys. J. R. Astron. Soc. **63**, 515–532, 1980

Båth, M.: Spectral Anaysis in Geophysics. Amsterdam: Elsevier 1974

Boigk, H., Schoeneich, H.: Die Tiefenlage der Permbasis im noerdlichen Teil des Oberrheingrabens. In: Graben Problems, J. H. Illies and St. Mueller, eds.: pp 45–55. Stuttgart: Schweizerbart'sche Verlagsbuchhandlung 1968

Born, M.: Optik. Berlin: Springer 1933

Braile, L.W., Smith, R.B.: Guide to the interpretation of crustal refraction profiles. Geophys. J. R. Astron. Soc. **40**, 145–176, 1975

Braile, L.W.: Interpretation of crustal velocity gradients and Q structure using amplitude-corrected seismograms. In: The earth's crust. Am. Geophys. Union Monogr. **20**, 427–439, 1977

Braile, L.W., Smith, R.B., Ansorge, J., Baker, M.R., Sparlin, M.A., Prodehl, C., Schilly, M.M., Healy, J.H., Mueller, St., Olsen, K.H.: The Yellowstone-Snake River Plain seismic profiling experiment: Crustal structure of the Eastern Snake River Plain. J. Geophys. Res. **87**, 2597–2610, 1982

Buechi, U.P., Lemcke, K., Wiener, G., Zimdars, J.: Geologische Ergebnisse der Erdoelexploration auf das Mesozoikum im Un-

tergrund des schweizerischen Molassebeckens. Bull. Ver. Schweiz. Petrol. Geol. Ing. **32**, 82, 7–38, 1965

Chapman, C.H.. A new method for computing synthetic seismograms. Geophys. J. R. Astron. Soc. **54**, 481–518, 1978

Červený, V.: On dynamic properties of reflected and head waves in n-layered earth's crust. Geophys. J. R. Astron. Soc. **11**, 139–147, 1966

Červený, V.. Accuracy of ray theoretical seismograms. J. Geophys. **46**, 135–149, 1979

Červený, V., Molotkov, I.A., Pšenčik, I.. Ray method in seismology. Prague: Charles University Press 1977

Fauria, T.J.: Crustal structure of the Northern Basin and Range and Snake River Plain: A ray-trace travel-time interpretation of the Eureka, Nevada, to Boise, Idaho, seismic refraction profile. M.S. Thesis, Purdue University 1981

Fuchs, K.: The reflection of spherical waves from transition zones with arbitrary depth-dependent elastic moduli and density. J. Phys. Earth **16** (Spec. Issue), 27–41, 1968

Fuchs, K., Müller, G.: Computation of synthetic seismograms with the reflectivity method and comparison with observations. Geophys. J. R. Astron. Soc. **23**, 417–433, 1971

Gebrande, H.: A seismic-ray tracing method for two-dimensional inhomogeneous media. In: Explosion seismology in central europe, P. Giese, C. Prodehl and A. Stein, eds.: pp. 162–167. Heidelberg: Springer 1976

Healy, J.H. Crustal structure along the coast of California from seismic-refraction measurements. J. Geophys. Res. **68**, 5777–5787, 1963

Hill, D.P.. Velocity gradients and anelasticity from crustal body wave amplitudes. J. Geophys. Res. **80**, 3309–3325, 1971

Hill, D.P., Pakiser, L.C.: Crustal structure between the Nevada test site and Boise, Idaho, from seismic-refraction measurements. In: The Earth beneath the continents, Am. Geophys. Union Monogr. **10**, 391–419, 1966

Kind, R.: The reflectivity method for a buried source. J. Geophys. **44**, 603–612, 1978

Lemcke, K., Buechi, U.P., Wiener, G.: Einige Ergebnisse der Erdoelexploration auf die mittellaendische Molasse der Zentralschweiz. Bull. Ver. Schweiz. Petrol. Geol. Ing. **35**, 87, 15–34, 1968

Müller, G., Fuchs, K.: Inversion of seismic records with the aid of synthetic seismograms. In: Explosion seismology in Central Europe, P. Giese, C. Prodehl and A. Stein, eds.: pp. 178–188. Heidelberg: Springer 1976

Müller, G., Mueller, S.: Travel-time and amplitude interpretation of crustal phases on the refraction profile Delta-W, Utah. Bull. Seismol. Soc. Am. **69**, 1121–1132, 1979

Olsen, K.H., Keller, G.R., Stewart, J.N.: Crustal structure along the Rio Grande Rift from seismic refraction profiles. In: Rio Grande Rift: Tectonics and magmatism, R.E. Riecker, ed.: pp. 127–143. Washington: Am. Geophys. Union 1979

Prodehl, C.: Seismic refraction study of crustal structure in the Western United States. Geol. Soc. Am. Bull. **81**, 2629–2646, 1970

Prodehl, C.: Crustal structure of the Western United States. U.S. Geol. Surv. Professional Paper **1034**, 18–23, 1979

Smith, R.B., Braile, L.W., Keller, G.R.: Upper crustal low-velocity layer: a possible effect of high temperatures over a mantle upward at the Basin and Range-Colorado Plateau transition. Earth Planet. Sci. Lett. **28**, 197–204, 1975

Spudich, P., Orcutt, J.: A new look at the seismic velocity structure of the Oceanic Crust. Rev. Geophys. Space Phys. **18**, 3, 627–645, 1980

Wiggins, R.A.: Body wave amplitude calculation-II. Geophys. J. R. Astron. Soc. **46**, 1–10, 1976

Received May 6, 1982; Revised version July 9, 1982
Accepted July 12, 1982